Journal of Solid State Chemistry 187 (2012) 143–148

Contents lists available at SciVerse ScienceDirect

Journal of Solid State Chemistry

journal homepage: www.elsevier.com/locate/jssc

Versatile lanthanide-azide complexes with azide/carboxylate/hydroxy mixed bridged chain exhibiting magnetic and luminescent properties

Hai-Chao Wang [a], Min Xue [a], Qian Guo [a], Jiong-Peng Zhao [a,*], Fu-Chen Liu [a,b,*], Joan Ribas [c]

[a] School of Chemistry and Chemical Engineering, Tianjin University of Technology, Tianjin 300384, PR China
[b] Lanzhou Petrochemical College of Vocational Technology 730060, PR China
[c] Inorgànica Universitat de Barcelona, Diagonal, 6487, 08028-Barcelona, Spain

ARTICLE INFO

Article history:
Received 4 July 2011
Received in revised form
1 December 2011
Accepted 26 December 2011
Available online 11 January 2012

Keywords:
Hydrothermal synthesis
Lanthanide-azide
Magnetism
Luminescence

ABSTRACT

Two new lanthanide-azide complexes, $[Ln_2(N_3)(isonic)_2(OH)_3(Hisonic)(H_2O)]_n$ (Ln=Yb for **1** and Tb for **2**, isonic=isonicotinate), were obtained in hydrothermal condition. X-ray diffraction analysis indicated the two complexes are isomorphic chain structure in which the Ln^{III} ions are mixed bridged by the azide anions, hydroxyl anions and carboxylate groups of the isonicotinate ligands. Further studies indicated weak antiferromagnetic interactions between the Ln^{III} ions in **1** and **2**, and complex **2** exhibit green sensitized Luminescent character of Tb^{III} ion.

1. Introduction

Metal azide complexes have drawn much attentions for their divertive structures and properties [1,2]. Azide ions could bridge metal ions in different ways derived from two basic modes EE (end to end) and EO (end on)[3,4]. Plentiful metal-azide complexes from 0D discrete to 3D framework have been prepared with attractive structures and particular properties [5]. However, the most metal-azide complexes are based on 3d transition metal ions; other metal-azide complexes are heavy explosive, so the isolation and handling of them bring considerable challenges to experimentalists [6]. In the literature some azide complexes based on main group elements and heavy metal ions were reported [7]. As kinds of heavy metal complexes the lanthanide-azide complexes are slowly developed and only several examples were reported since the first lanthanide-azide compound was obtained in 1988 [8]. So exploring new assembling methods to avoid the potential explosive in the lanthanide-azide complexes is significant in gaining new lanthanide complexes as well as their properties studying [8,9]. In order to obtain thermally stable metal-azide complexes, co-ligands were often introduced. Comparing with other synthesized methods, hydrothermal synthesis reaction is simple, fast and efficient (typically response time is shorter, each can have multiple response), low cost and less pollution. Those characters make it a good choice to synthesize metal-azide complexes with certainly co-ligands. Here, we report the synthesis, structure and properties of two new 1D lanthanide-azide complexes $Ln_2O_4N_3(isonic)_3$ (Ln=Yb for **1** and Ln=Tb for **2**) with isonicotinatic as co-ligand obtained by hydrothermal reactions. Magnetic and emission spectrum studies indicated domain antiferromagnetic coupling between the Yb^{III} ions of **1** and green sensitized luminescent character of Tb^{III} in **2**.

2. Experimental section

2.1. Materials and general methods.

All the reagents for synthesis were obtained commercially and used as received. Elemental analyses of C, H and N were performed on a Perkin–Elmer 240C analyzer. The FT-IR spectra were recorded from KBr pellets in the range $4000-400\,cm^{-1}$ on a TENSOR 27 (Bruker) spectrometer. The X-ray powder diffraction (XRPD) was recorded on a Rigaku D/Max-2500 diffractometer at 40 kV, 100 mA for a Cu-target tube and a graphite monochromator. Simulation of the XRPD spectra was carried out by the single-crystal data and diffraction-crystal module of the Mercury (Hg) program available free of charge via the Internet at http://www.iucr.org. Magnetic data were collected using crushed crystals of the sample on a Quantum Design MPMS XL-7 SQUID magnetometer. Solid-state

* Corresponding authors.
E-mail addresses: horryzhao@yahoo.com (J.-P. Zhao), fuchenliutj@yahoo.com (F.-C. Liu).

0022-4596/$ - see front matter © 2012 Elsevier Inc. All rights reserved.
doi:10.1016/j.jssc.2011.12.038

emission and excitation spectra of compounds were measured using a Cary Eclips fluorescence spectrophotometer.

2.2. Synthesis of complexes

A mixture of $Ln(NO_3)_3 \cdot 6H_2O$ (2 mmol) (Ln=Yb for **1** and Ln=Tb for **2**), NaN_3(1 mmol), Hnic (2 mmol) and H_2O (15 ml) was sealed in a Teflon-lined autoclave and heated to 140 °C for 2 d and cooled to room temperature at 10 °C h^{-1}. The crystals were obtained in ca. 20% yield based on metal used. Anal. calcd for $C_{18}H_{18}Yb_2N_6O_{10}$ (**1**): C, 26.22; H, 2.20; N, 10.19%. Found: C, 26.41; H, 2.50; N, 10.43%. Anal. Calcd for $C_{18}H_{18}Tb_2N_6O_{10}$ (**2**): C, 27.15; H, 2.29; N, 10.55%. Found: C, 27.45; H, 2.34; N, 10.79%. IR (KBr pellet, cm^{-1}) of **1** and **2** see Fig. S1 in Supplementary data.

Caution! Azide complexes are potentially explosive. Only a small amount of the materials should be prepared and handled with care.

Table 1
Crystal data and structure refinement parameters for complexes **1** and **2**.

	1	**2**
Chemical formula	$C_{18}H_{18}Yb_2N_6O_{10}$	$C_{18}H_{18}Tb_2N_6O_{10}$
Formula weight	824.46	796.22
Space group	*P-1*	*P-1*
a (Å)	7.0938(14)	8.0431(16)
b (Å)	12.415(3)	12.542(3)
c (Å)	12.492(3)	12.567(3)
α (deg)	108.88(3)	108.24(3)
β (deg)	97.89(3)	104.16(3)
γ (deg)	102.05(3)	98.02(3)
V (Å^3)	992.8(3)	1134.9(4)
Z	2	2
D (g cm^{-3})	2.758	2.330
μ (mm^{-1})	9.440	6.249
T (K)	293(2)	293(2)
R [a]/wR [b]	0.0570 /0.859	0.0492/0.0754

[a] $R=\Sigma||F_o| - |F_c|| / \Sigma|F_o|$;
[b] $R_w=[\Sigma[w(F_o^2 - F_c^2)^2] / \Sigma w(F_o^2)^2]^{1/2}$.

2.3. X-ray data collection and structure determinations.

Single-crystal X-ray diffraction measurements for **1** and **2** were carried out on a Bruker Smart 1000 CCD diffractometer equipped with a graphite crystal monochromator situated in the incident beam. The determinations of unit cell parameters and data collections were performed with Mo-$K\alpha$ radiation (λ=0.71073 Å) at 294(2) K and unit cell dimensions were obtained with least-squares refinements. The program SAINT [10] was used for integration of the diffraction profiles. All the structures were solved by direct methods using the SHELXS program of the SHELXTL package and refined by full-matrix least-squares methods with SHELXL (semi-empirical absorption corrections were applied using SADABS program) [11]. Metal atoms in each complex were located from the *E*-maps and other non-hydrogen atoms were located in successive difference Fourier syntheses and refined with anisotropic thermal parameters on F^2. The hydrogen atoms of the ligands were generated theoretically onto the specific atoms and refined isotropically with fixed thermal factors. Crystallographic data (excluding structure factors) for **1** and **2** have also been deposited on the Cambridge Crystallographic Data Centre as supplementary publication (no. CCDC-794801 and 794802). Copies of the data can be obtained free of charge on application to CCDC, 12 Union Road, Cambridge CB21EZ, UK (fax: (+44) 1223-336-033; e-mail: deposit@ccdc.cam.ac.uk). Details of the X-ray crystal structure analysis of **1** and **2** are summarized in Table 1.

3. Results and discussion

3.1. Structure descriptions of complexes 1 and 2.

The two complexes are isomorphous crystallizing in the space group P-1, therefore only the structure of **2** was described in detail. The asymmetric unit of **2** contains two Tb^{III} , one azide, three hydroxyl anions, one coordinated water molecule, one Hisonic molecule and two isonic anions, in which the Tb^{III} ions are all eight coordinated with an anti-prismatic geometry. Tb1 ion

Table 2
Selected bond lengths (Å) and angles for complexes **1** and **2** [deg].

1		2	
Yb(1)–O(8)	2.149(5)	Tb(1)–O(1)	2.333(5)
Yb(1)–O(9)	2.180(5)	Tb(1)–O(9)	2.352(4)
Yb(1)–O(1)#1	2.243(6)	Tb(1)–O(3)	2.356(5)
Yb(1)–O(3)#1	2.265(6)	Tb(1)–O(9)	2.365(4)
Yb(1)–N(1)	2.303(8)	Tb(1)–O(8)#2	2.391(4)
Yb(1)–O(9)#2	2.315(6)	Tb(1)–O(1 W)	2.420(5)
Yb(1)–O(1W)	2.369(6)	Tb(1)–N(1)	2.502(6)
Yb(1)–O(7)	2.380(6)	Tb(1)–O(7)	2.555(4)
Yb(2)–O(9)	2.179(5)	Tb(2)–O(4)#3	2.332(5)
Yb(2)–O(8)#3	2.185(5)	Tb(2)–O(2)#3	2.343(5)
Yb(2)–O(4)	2.236(7)	Tb(2)–O(6)	2.344(5)
Yb(2)–O(2)	2.248(7)	Tb(2)–O(8)	2.370(4)
Yb(2)–N(1)	2.284(7)	Tb(2)–O(9)#2	2.400(4)
Yb(2)–O(6)	2.296(7)	Tb(2)–O(8)#4	2.410(4)
Yb(2)–O(8)#2	2.314(6)	Tb(2)–N(1)	2.457(6)
Yb(2)–O(7)	2.399(6)	Tb(2)–O(7)	2.551(5)
Yb(2)–O(9)–Yb(1)	98.7(2)	Tb(1)#2–O(9)–Tb(1)	107.60(17)
Yb(2)–O(9)–Yb(1)#2	108.3(2)	Tb(1)#2–O(9)–Tb(2)#2	104.65(16)
Yb(1)–O(9)–Yb(1)#2	109.0(2)	Tb(1)–O(9)–Tb(2)#2	108.02(17)
Yb(1)–O(7)–Yb(2)	87.6(2)	Tb(2)–O(7)–Tb(1)	94.89(15)
Yb(2)–N(1)–Yb(1)	92.3(3)	Tb(2)–N(1)–Tb(1)	98.6(2)
Yb(1)–O(8)–Yb(2)#1	122.2(3)	Tb(2)–O(8)–Tb(1)#2	108.13(17)
Yb(1)–O(8)–Yb(2)#2	109.4(2)	Tb(2)–O(8)–Tb(2)#4	105.45(16)
Yb(2)#1–O(8)–Yb(2)#2	106.9(2)	Tb(1)#2–O(8)–Tb(2)#4	126.62(18)
#1 $x+1,y,z$ #2 $-x+1,-y+1,-z+1$ #3 $x-1,y,z$		#2 $-x+1,-y+1,-z+1$ #3 $x+1,y,z$ #4 $-x+2,-y+1,-z+1$	

is coordinated with one nitrogen atom [Tb1–N1=2.502(6) Å] from an azide anion, two oxygen atoms [Tb1–O1=2.333(5) Å, Tb1–O3=2.356(5) Å] from two isonic groups, one μ_2 hydroxyl group [Tb1–O7= 2.555(5) Å], three μ_3 hydroxyl groups [Tb1–O8B=2.391(4) Å , Tb1–O9=2.365(5) Å , Tb1–O9B=2.352(4) Å] and a water molecule [Tb1–O1W=2.421(5) Å]. Tb2 is coordinated by an azide nitrogen atom [Tb2–N1=2.457(6) Å], three oxygen atoms [Tb2–O2C=2.343(5) Å, Tb2–O4C=2.332(5) Å, Tb2–O6= 2.344(5) Å] from two isonic and a Hisonic, respectively, one μ_2 hydroxyl group [Tb2–O7=2.553(5) Å] and three μ_3 hydroxyl groups [Tb2–O8=2.370(5) Å, Tb2–O8D=2.410(4) Å , Tb2–O9B= 2.400(5) Å]. The selected bonds length and angles of **1** and **2** are shown in the Table 2. As shown in Fig. 1, the azide anions take EO mode to bridgeTb1 and Tb2 forming a dimmer. The isonic ligands and hydroxyl groups act in two modes, bi-dentate μ_2-O,O (*syn–syn*)

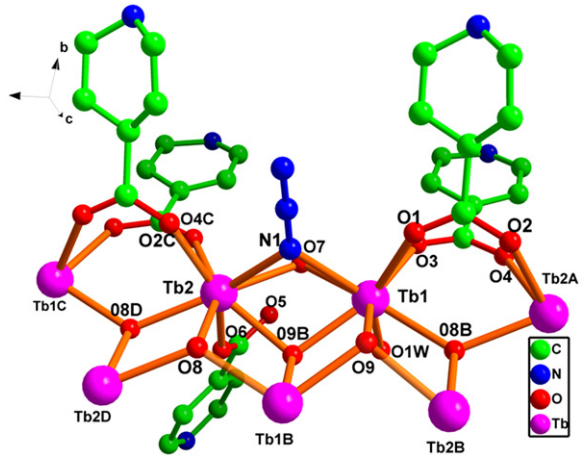

Fig. 1. Coordination and linkage modes of ligands and Tb^{III} ions in complex **2**.

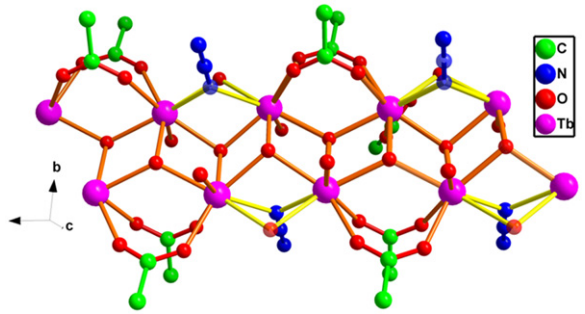

Fig. 2. One dimensional chain of complex **2**, pyridyl groups were omitted for clarify.

and mono-dentate for isonic, μ_2 and μ_3 model for the hydroxyl groups. The metal azide dimmers were connected by the hydroxyl groups giving a 1D chain. As shown in Fig. 2, the skeleton of the one-dimensional chain is a wave-like ladder (shown by orange) constructed by Tb ions and μ_3 hydroxyl, which is reinforced between adjacent Tb^{III} ion of two manners: one is coordinated bonds formed by two carboxylate groups of isonic with *syn–syn* mode shown by turquoise, and the other is the linkage of the μ_2 hydroxyl anions and a $\mu_{1,1}$ azide anions shown in gold. It is interesting that intra-chain and inter-chain H-bonds were found in the complex (Table 3). Intra-chain H-bonds between the hydroxyl group O7 and the oxygen atom O5 form the carboxylate group of isonic anions were found. And inter-chains H-bond were also found between O7 and the protoned nitrogen atom of the Hisonic ligand. Beside that the coordinated water molecule formed two inter-chain H-bonds with the nitrogen atoms of the isonic anions in the neighbor chains. Thus, the 1D chain was connected to neighbors by the inter-chain H-bond forming a 3D super molecule structure (Fig. 3).

3.2. Magnetic properties.

Magnetic measurements were carried out on crystalline samples of complexes **1** and **2** which were pure-phase (confirmed by XRPD, see (Fig. S2). The magnetic susceptibilities of **1** and **2** were collected in the 2–300 K temperature range under 1 kOe. Owing to two factors, the spin-orbit coupling of the Ln^{III} ions and the complicated structure of the complexes, any attempt to try to fit the magnetic data will be unsuccessful. Only an estimation of the magnetic coupling can be drawn from the experimental data. Considering the structure, there are many magnetic pathways between the Ln^{III} ions in the two-dimensional network: *syn–syn*-carboxylate bridges, μ_2-oxo bridges, μ_3-oxo bridges and μ-N_3 (end-on) bridges. Usually, very weak ferro- or antiferromagnetic interactions should be conducted by those bridges except the end-on azide ligands [12]. There is less magnetism-structure study in lanthanide complexes with azido anions as bridge [13], while the end-on azide anions conduct practically strong ferromagnetic coupling between 3d metal ions [6]. Anyway, the interactions conducted by the bridges between the Ln^{III} ions are very weak.

Plots of χ_m and $\chi_m T$ vs T of **1** are shown in Fig. 4(a). The $\chi_m T$ curve starts at 2.52 $cm^3\ mol^{-1}$ K, which is the typical value for the free Yb^{III} ion at room temperature. The $\chi_m T$ values decrease monotonously to 1.3 $cm^3\ mol^{-1}$ K at 2 K. This monotonous decreasing is not the conventional, mainly at high temperature, for isolated Yb^{III} complexes. The ground manifold of free-ion Yb^{III} is $^2F_{7/2}$ ($S=1/2$; $L=3$, $J=7/2$) with only one excited level, $^2F_{5/2}$. Since the excited level is about 10,000 cm^{-1}, not only is there no population of this level, but also there is essentially no second

Table 3
Hydrogen-bond geometry (Å, °) for complexes **1** and **2**.

D–H···*A*	*D*–H	H···*A*	*D*···*A*	*D*–H···*A*
1				
O7–H7···O5	0.85	1.81	2.629 (9)	162
O1*W*–H1 *WA*···N4^{v}	0.85	1.96	2.773 (10)	161
O1 *W*–H1*WB*···N6^{vi}	0.85	2.30	2.826 (11)	121
N5–H5*B*···O7^{vii}	0.96	1.87	2.783 (11)	158
Symmetry codes: (v) −x+2, −y, −z+1; (vi) −x+2, −y, −z; (vii) −x+2, −y+1, −z.				
2				
O7–H7···O5	0.82 (6)	1.93 (6)	2.700 (7)	158 (6)
O1*W*–H1*WA*···N4^{vii}	0.85	1.98	2.784 (8)	158
O1*W*–H1*WB*···N6^{vi}	0.85	1.97	2.811 (8)	168
N5–H5*B*···O7^{v}	0.90	1.91	2.799 (8)	169
Symmetry codes: (v) −x+1, −y+2, −z+1; (vi) −x+1, −y+2, −z+2; (vii) −x+2, −y+1, −z+2.				

order Zeeman effect between excited and ground level [12]. The energy level diagram of the $^2F_{7/2}$ manifold is also internally very simple. In cubic symmetry the manifold is split into three multiplets, Γ_7, Γ_8 and Γ_6 (representations of the cubic double group). A simplification is that within the $J=7/2$ manifold, Γ_7, the ground state is separated from Γ_8, the first excited multiplet, by 550 cm^{-1}, approximately. The Γ_6 is even higher. From this it follows that in a first approximation only the Γ_7 is populated at room temperature and below. In that approximation Γ_8 contributes only via the second-order Zeeman effects [14]. The $^2F_{7/2}$ ground state predicts a magnetic moment of 4.5 $N\beta$ ($\chi_m T=2.57$ cm^3 mol^{-1} K) [15]. Usually, the average moment of Yb^{III} salts, such as in $Yb_2(SO_4)_3 \cdot 8H_2O$ remains nearly constant between 300 K and 100 K [15], and the magnetization vs. H at 2 K follows the Brillouin function with a saturation value about 4 $N\beta$ ($M=gJN\beta$, $g=8/7$ and $J=7/2$) [14–16]. However in the most case the situation is much complicated. The $^{2S+1}\Gamma_J$ ground state is partially split by the ligand field [15]. And in the case of the Kramers doublets (half-integer J) the multiplet width of such splitting may vary from a few tens to few hundreds of mave-numbers [15,17]. The components of higher energy are successively depopulated with the temperature is lowered. Thus, the $^{2S+1}\Gamma_J$ ground state being statistically populated at room temperature becomes less valid. In this complex the $\chi_m T$ values have monotonous decreasing with the cooling indicates that noticeable antiferromagnetic coupling is inherent to the structure or the partially splitting of the ground state by the ligand field. However, in conventional situation the interactions between the 4f elements Ln^{III} ions are very weak, thus, the ligand field may govern the decreasing of the $\chi_m T$ with cooling primarily. The plot of the reduced magnetization corroborates this fact: at 2 K the saturation value of complex **1** this value is only close to 2 $N\beta$ (Fig. 4(b)) far from 4 $N\beta$. This difference, apart from antiferromagnetic coupling

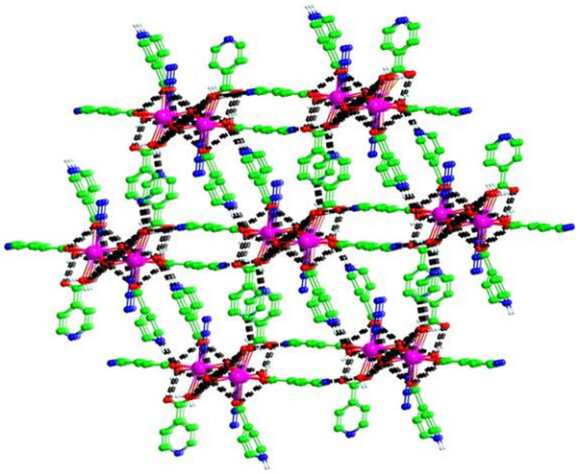

Fig. 3. The packing mode of complex **2** along *c* direction with the H-bonds labeled in black.

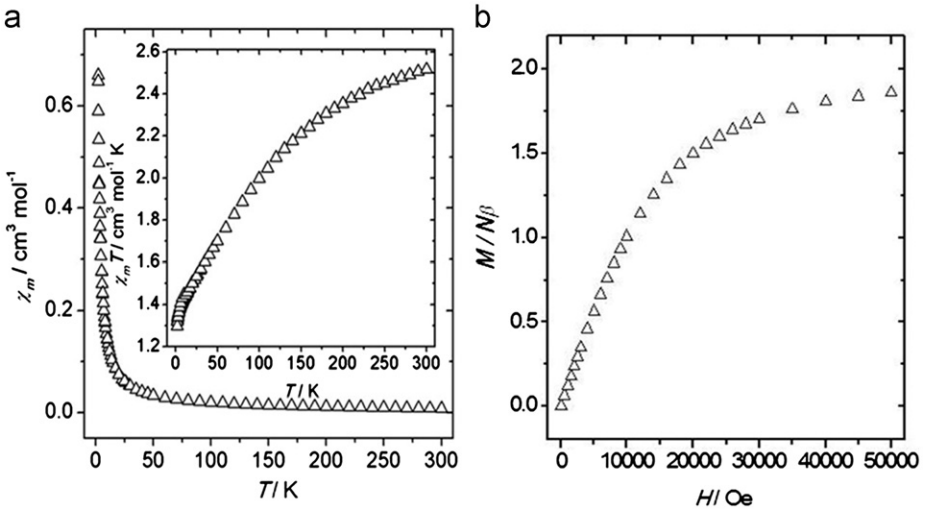

Fig. 4. (a) Plot of the χ_m and $\chi_m T$ (inset) vs T for complex **1** (account for one Yb^{III} ions). (b) Plot of the reduced magnetization (M / $N\mu_\beta$) at 2 K for **1**.

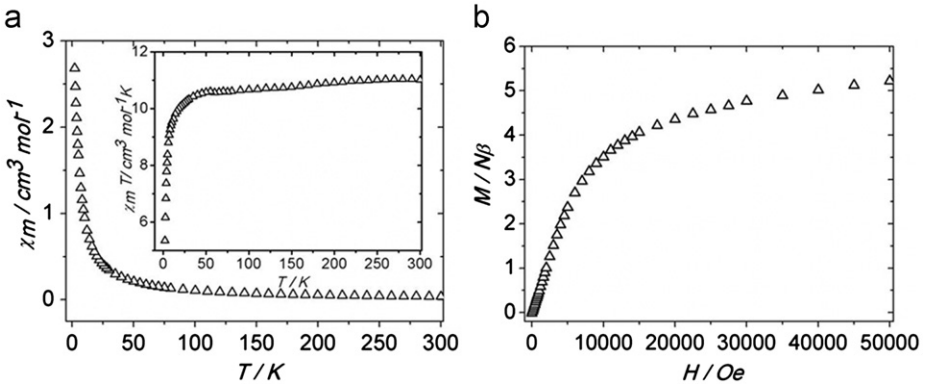

Fig. 5. (a) Plot of the χ_m and $\chi_m T$ (inset) vs T for complex **2** (account for one Tb^{III} ions). (b) Plot of the reduced magnetization (M / $N\mu_\beta$) at 2 K for **2**.

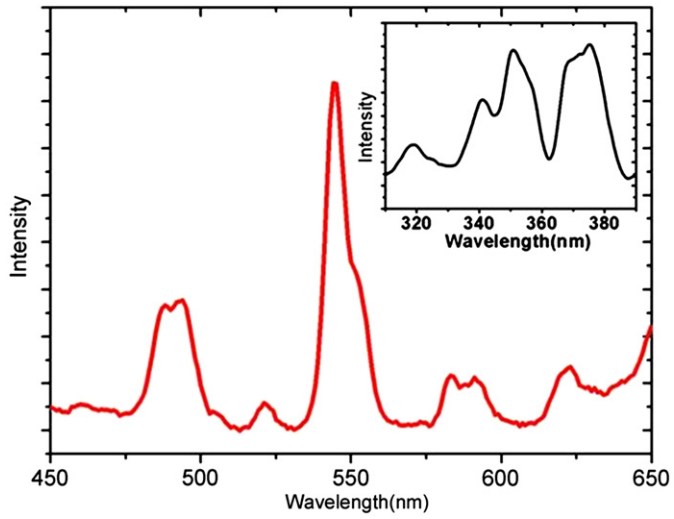

Fig. 6. Emission spectrum of the complex **2**. Insert: the excitation spectra of **2** in the solid state.

is indicative anisotropy of the complex associated with splitting of the ground state which results in a typical experimental value of the magnetization 2 $N\mu_B$ for one Yb^{III} ion [18].

The plots of χ_m and $\chi_m T$ vs. T of **2** are shown in Fig. 5(a). The $\chi_m T$ curve starts at 11.02 $cm^3\ mol^{-1}$ K, which is the typical value for the free Tb^{III} ion ($^7F_6$) at room temperature. Starting from room temperature, $\chi_m T$ values are practically constant to 50 K and below 50 K they decrease quickly to 2.02 $cm^3\ mol^{-1}$ K at 2 K. This feature is characteristic of very weak antiferromagnetic interactions. The magnetization $M/N\beta$ value at 2 K under 5 T is 5.22 $N\beta$ does not reach the expected saturation of 9 $N\beta$ for one Tb^{III} ion due to the ligands field effect on the Tb^{III} ion as well as very small antiferromagnetic coupling (Fig. 5(b)).

3.3. Luminescence properties.

It is known that many lanthanide metal compounds exhibit luminescent properties and the ligands of could improve sensitization of the lanthanide complexes the complex [19]. In the lanthanide complexes the Tb^{III} and Eu^{III} could produce luminescence in the visible region, while Nb^{III}, Er^{III} and Yb^{III} are capable of emission in the near-infrared region [20]. The luminescent properties of complexes **1** and **2** were measured in the solid state at room temperature. When excited at 310 nm which could be attributed to intraligand (isonicotinate) charge transfer (n-π^* or π-π^*), complex **1** exhibits a ligand emission band at 498 nm (Fig. S3). And the luminescence of Yb^{III} in the near-infrared region need further study. The excitation of **2** in the solid state shows two obvious energy bands in the UV region 350 nm and 378 nm with emission band 544 nm (Fig. 6 insert). The emission spectrum displays the green luminescence characteristic of Tb^{III} ions upon exposure to both at 350 nm (Fig. 6) and 378 nm (Fig. S4) UV radiations. The intense emission band at 544 nm corresponds to $^5D_4 \rightarrow {}^7F_5$ transitions, while the weak emission bands at 490, 584, 621 nm originate from $^5D_4 \rightarrow {}^7F_6$, $^5D_4 \rightarrow {}^7F_4$, and $^5D_4 \rightarrow {}^7F_3$ transitions, respectively.

4. Conclusion

In summary the structure and properties studies of the two new lanthanide-azide complexes synthesized by hydrothermal reaction were reported, which suggests that the synthesis strategy for the title compounds may open a new perspective way to generate lanthanide-azide complexes with versatile properties.

Acknowledgments

This work was supported by the National Natural Science Foundation of China (No. 20801041 and 21101114) and the Tianjin Municipal Education Commission (No. 20100502).

Appendix A. Supplementary materials

Supplementary materials associated with this article can be found in the online version at doi:10.1016/j.jssc.2011.12.038.

References

[1] (a) W.J. Evans, K.A. Miller, J.W. Ziller, J. Greaves, Inorg. Chem. 46 (2007) 8008–8018;
(b) W.J. Evans, E. Montalvo, T.M. Champagne, J.W. Ziller, A.G. DiPasquale, A.L. Rheingold, J. Am. Chem. Soc. 130 (2008) 16–17.
[2] (a) G.F. Zi, L. Jia, E.L. Werkema, M.D. Walter, J.P. Gottfriedsen, R.A. Andersen, Organometallics 24 (2005) 4251–4264;
(b) G. Nocton, J. Pécaut, M. Mazzanti, Angew. Chem. Int. Ed. 47 (2008) 3040–3042;
(c) J.P. Zhao, B.W. Hu, X.F. Zhang, Q. Yang, M.S. El Fallah, J. Ribas, X.H. Bu, Inorg. Chem. 49 (2010) 1325–1332.
[3] (a) U.P. Singh, S. Tyagi, C.L. Sharma, H. Görner, T. Weyhermüller, J. Chem. Soc., Dalton Trans. (2002) 4464–4470;
(b) J. Ribas, M. Monfort, R. Costa, X. Solans, Inorg. Chem. 32 (1993) 695–699;
(c) A. Escuer, R. Vicente, M.S. El Fallah, J. Ribas, X. Solans, M. Font-Bardia, Dalton Trans. (1993) 2975–2976;
(d) R. Cortes, M.K. Urtiaga, L. Lezama, J.L. Pizarro, A. Goni, M.I. Arriortua, T. Rojo, Inorg. Chem. 33 (1994) 4009–4015.
[4] (a) J.P. Zhao, B.W. Hu, E.C. Sañudo, Q. Yang, Y.F. Zeng, X.H. Bu, Inorg. Chem. 48 (2009) 2482–2489;
(b) J.P. Zhao, B.W. Hu, Q. Yang, X.F. Zhang, T.-L. Hu, X.H. Bu, Dalton Trans. 39 (2010) 56–58.
[5] (a) M.J. Crawford, A. Ellern, P. Mayer, Angew. Chem., Int. Ed. 44 (2005) 7874–7878;
(b) F.C. Liu, Y.F. Zeng, J.P. Zhao, B.W. Hu, X.H. Bu, J. Ribas, J. Cano, Inorg. Chem. 46 (2007) 1520–1522;
(c) W.J. Evans, S.A. Kozimor, J.W. Ziller, Science 309 (2005) 1835–1838;
(e) J. Boonmak, M. Nakano, N. Chaichit, C. Pakawatchai, S. Youngme, Inorg. Chem. 50 (2011) 7324–7333;
(f) Y.L. Zhou, M.H. Zeng, L.Q. Wei, B.W. Li, M. Kurmoo, Chem. Mater. 22 (2010) 4295–4303;
(g) M.H. Zeng, Y.L. Zhou, W.X. Zhang, M. Du, H.L. Sun, Cryst. Growth Des. 10 (2010) 20–24.
[6] (a) Y.F. Zeng, X. Hu, F.C. Liu, X.H. Bu, Chem. Soc. Rev. 38 (2009) 469–480;
(b) J. Müller, Coord. Chem. Rev. 235 (2002) 105–119.
[7] (a) A. Villinger, A. Schulz, Angew. Chem. Int. Ed. 49 (2010) 8017–8020;
(b) P. Portius, A.C. Filippou, G. Schnakenburg, M. Davis, K.-D. Wehrstedt, Angew. Chem. Int. Ed. 49 (2010) 8013–8016.
[8] (a) H. Schumann, C. Janiak, J. Pickardt, J. Organomet. Chem. 349 (1988) 117–122;
(b) R. Kumar, U.P. Singh, J. Mol. Struct. 875 (2008) 427–434;
(c) F.C. Liu, Y.F. Zeng, J.P. Zhao, B.W. Hu, X. Hu, J. Ribas, X.H. Bu, Dalton Trans. (2009) 2074–2076;
(d) R. Sen, S. Koner, D.K. Hazra, M. Helliwell, M. Mukherjee, Eur. J. Inorg. Chem. (2011) 241–248.
[9] (a) D. Parker, Coord. Chem. Rev. 205 (2000) 109–130;
(b) V.W.W. Yam, K.K.W. Lo, Coord. Chem. Rev. 184 (1999) 157–240.
[10] A.X.S. Bruker, SAINT Software Reference Manual, Madison: WI, 1998.
[11] (a) G.M. Sheldrick, SADABS, Siemens Area Detector Absorption Corrected Software, University of Göttingen, Germany, 1996;
(b) G.M. Sheldrick, N.T. SHELXTL, Version 5.1. Program for Solution and Refinement of Crystal Structures, University of Göttingen, Germany, 1997.
[12] (a) X.J. Zheng, L.P. Jin, S. Gao, Inorg. Chem. 43 (2004) 1600–1602;
(b) Y. Wan, L. Zhang, L. Jin, S. Gao, S. Lu, Inorg. Chem. 42 (2003) 4985–4994;
(c) T.F. Liu, J. Lu, C. Tian, M. Cao, Z. Lin, R. Cao, Inorg. Chem. 50 (2011) 2264–2271.
[13] (a) J. Rinck, G. Novitchi, W.V. den Henuvel, L. Unger, Y. Lan, W. Wernsdorfer, C.E. Anson, L.F. Chibotaru, A.K. Powell, Angew. Chem. Int. Ed. Engl. 49 (2010) 7583;

(b) C.E. Burrow, T.J. Burchell, P.H. Lin, W. Wernsdorfer, R. Clerac, M. Murugeru, Inorg. Chem. 48 (2009) 8051.
[14] T.H. Siddall, in: E.A. Boudreaux, L.N. Mulay (Eds.), Theory and Applications of Molecular Paramagnetism, Jonh-Wiley & Sons, New York, 1976. Chapter 4.
[15] O. Kahn, Molecular Magnetism, VCH, New York, 1993. Chapter 3.
[16] A.T. Casey, S. Mitra, in: E.A. Boudreaux, L.N. Mulay (Eds.), Theory and Applications of Molecular Paramagnetism, Jonh-Wiley & Sons, New York, 1976. Chapter 5.
[17] M.A. AlDamen, S. Cardona-Serra, J.M. Clemente-Juan, E. Coronado, A. Gaita-Ariño, C. Martí-Gastaldo, F. Luis, O. Montero, Inorg. Chem. 48 (2009) 3467–3479.
[18] A. Figuerola, C. Diaz, J. Ribas, V. Tangoulis, C. Sangregorio, D. Gatteschi, M. Maestro, Mahía José, Inorg. Chem. 42 (2003) 5274–5281.
[19] S. Viswanathan, A. Bettencourt-Dias, Inorg. Chem. 45 (2006) 10138–10146.
[20] X.P. Yang, R.A. Jones, M.M. Oye, A.L. Holmes, W.K. Wong, Cryst. Growth Des. 6 (2006) 2122–2125.